Termination and Transfer Reactions in the Group Transfer Polymerizations of Acrylates Catalyzed by Mononuclear Early d-Block and f-Block Metallocenes: A DFT Study

Simone Tomasi,[†] Horst Weiss,[‡] and Tom Ziegler*[,†]

Department of Chemistry 2500, University of Calgary, University Drive, NW, Calgary, Alberta, Canada T2N1N4, and BASF Aktiengesellschaft, GKP/M−G200 67056, Ludwigshafen, Germany

Received November 17, 2006

The group transfer polymerization (GTP) of acrylates with early d-block and f-block metallocenium ester enolates suffers from side reactions, which cause the process not to be living, with a lack of control of the number-average molecular weight, molecular weight distribution, and tacticity, as well as an incomplete monomer conversion at low catalyst loadings. GTP of acrylates has so far met with limited success, due to the presence of a proton on the α-carbon, which provides low steric protection to the enolate in the unwanted backbiting reaction. Furthermore, the proton on the α-carbon is relatively acidic and therefore can be transferred. The computational study with the BP86 DFT functional of the backbiting and proton transfer reactions on realistic models for acrylate GTP provides detailed information on the mechanisms and hints on how to tailor the existing catalysts in order to minimize the unwanted side reactions.

Introduction

The group transfer polymerization (GTP) of methacrylates by group IV metallocenes and related compounds has attracted much attention in the scientific community since the seminal and independent works of Yasuda et al.,[1−3] Collins et al.,[4,5] and Boffa et al.,[6] dating back to the beginning of the 1990s. It constitutes a valid alternative to the traditional radical polymerizations because of the improved control it provides over important polymer properties such as number-average molecular weight, molecular weight distribution, and tacticity.[7−12] It has been shown by experimental[13,14] and theoretical[11,15−17] studies that acrylate and methacrylate GTP using group IV and related metallocenium ester enolates can proceed via a mononuclear or a binuclear mechanism. It can further be living,[7,13,18,19] thus also providing access to block copolymers when suitable catalyst systems are employed.[2,7,20−25] In the case of cationic zirconocene ester enolates, it has been shown that the GTP mechanism is the same as that postulated for the isoelectronic samarocene ester enolate first studied by Yasuda and co-workers.[21,26]

Unfortunately, the GTP of acrylates with zirconocenium ester enolates has so far met with much less success, compared to the polymerization of methacrylates. The principal reason that the GTP is much more successful with methacrylates than with acrylates is that the latter suffers from a number of unwanted side reactions caused by the presence of an acidic proton on the acrylate α-carbon as opposed to a methyl group in the case of methacrylates.

It has been shown that when *n*-butyl acrylate is polymerized using the bicomponent system of Collins, there are at least two side processes at higher temperatures, namely, backbiting and proton transfer,[13] and that backbiting occurs even at low temperatures. Backbiting causes termination, while proton transfer does not, although it contributes to widening the molecular weight distribution and likely slows the overall rate of polymerization. Similar processes are present in the polymerization of *n*-butyl acrylate catalyzed by cationic, mononuclear

* Corresponding author. E-mail: ziegler@ucalgary.ca.
† University of Calgary.
‡ BASF Aktiengesellschaft.

(1) Yasuda, H.; Yamamoto, H.; Yokota, K.; Miyake, S.; Nakamura, A. *J. Am. Chem. Soc.* **1992**, *114*, 4908.
(2) Yasuda, H.; Furo, M.; Yamamoto, H.; Nakamura, A.; Miyake, S.; Kibino, N. *Macromolecules* **1992**, *25*, 5115.
(3) Yasuda, H.; Yamamoto, H.; Yamashita, M.; Yokota, K.; Nakamura, A.; Miyake, S.; Kai, Y.; Kanehisa, N. *Macromolecules* **1993**, *27*, 7134.
(4) Collins, S.; Ward, D. G. *J. Am. Chem. Soc.* **1992**, *114*, 5460.
(5) Collins, S.; Ward, D. G.; Suddaby, K. H. *Macromolecules* **1994**, *27*, 7222.
(6) Boffa, L. S.; Novak, B. M. *Macromolecules* **1994**, *27*, 6993.
(7) Yasuda, H. *J. Organomet. Chem.* **2002**, *647*, 128.
(8) Nguyen, H.; Jarvis, A. P.; Lesley, M. J. G.; Kelly, W. M.; Reddy, S. S.; Taylor, N. J.; Collins, S. *Macromolecules* **2000**, *33*, 1508.
(9) Boffa, L. S.; Novak, B. M. *Chem. Rev.* **2000**, *100*, 1479.
(10) Frauenrath, H.; Keul, H.; Höcker, H. *Macromolecules* **2001**, *34*, 14.
(11) Hölscher, M.; Keul, H.; Höcker, H. *Chem.−Eur. J.* **2001**, *7*, 5419.
(12) Hölscher, M.; Keul, H.; Höcker, H. *Macromol. Rapid Commun.* **2000**, *21*, 1093.
(13) Li, Y.; Ward, D. G.; Reddy, S. S.; Collins, S. *Macromolecules* **1997**, *30*, 1875.
(14) Bandermann, F.; Ferenz, M.; Sustmann, R.; Sicking, W. *Macromol. Symp.* **2001**, *174*, 247.
(15) Sustmann, R.; Sicking, W.; Bandermann, F.; Ferenz, M. *Macromolecules* **1999**, *32*, 4204.
(16) Hölscher, M.; Keul, H.; Höcker, H. *Macromolecules* **2002**, *35*, 8194.
(17) Tomasi, S.; Weiss, H.; Ziegler, T. *Organometallics* **2006**, *25*, 3619.
(18) Stojcevic, G.; Kim, H.; Taylor, N. J.; Marder, T. B.; Collins, S. *Angew. Chem., Int. Ed.* **2004**, *43*, 5523.
(19) Bandermann, F.; Ferenz, M.; Sustmann, R.; Sicking, W. *Macromol. Symp.* **2001**, *174*, 247.
(20) Karanikolopoulos, G.; Batis, C.; Pitsikalis, M.; Hadjichristidis, N. *Macromolecules* **2001**, *34*, 4697.
(21) Rodriguez-Delgado, A.; Chen, E. Y.-X. *Macromolecules* **2005**, *38*, 2587.
(22) Rodriguez-Delgado, A.; Mariott, W. R.; Chen, E. Y.-X. *Macromolecules* **2004**, *37*, 3092.
(23) Ihara, E.; Morimoto, M.; Yasuda, H. *Macromolecules* **1995**, *28*, 7886.
(24) Chen, E. Y.-X.; Cooney, M. J. *J. Am. Chem. Soc.* **2003**, *125*, 7150.
(25) Bolig, A. D.; Chen, E. Y.-X. *J. Am. Chem. Soc.* **2002**, *124*, 5612.
(26) Rodriguez-Delgado, A.; Chen, E. Y.-X. *J. Am. Chem. Soc.* **2004**, *126*, 5612.

10.1021/om061058a CCC: $37.00
Publication on Web 03/27/2007

racemic zirconocenium ester enolates, as shown by Chen and co-workers.[27]

Acrylate GTP catalyzed by neutral samarocene ester enolates seems to suffer less from these shortcomings, allowing the production of poly(*n*-butyl acrylate) with high molecular weight and relatively narrow molecular weight distribution. However, also in this case it has been shown that the process is not stereospecific.[7,23]

The investigation of side reaction pathways in the GTP of acrylates is the subject of this paper. To our knowledge, only an experimental study on this topic has been published,[27] while no theoretical reports are yet available. Understanding the fine details of these processes is the first necessary step toward the design of modified catalysts, capable of polymerizing acrylic substrates more efficiently, without incurring low conversions and lack of control of the polymer properties. Possible beneficial modifications will be considered in the final part of this account.

Computational Details

Density functional theory (DFT) calculations on the systems of interest were carried out with the program ADF,[28,29] version 2004.01,[30] using the Becke−Perdew exchange−correlation functional (BP86).[31−33]

Double-ζ STO basis sets with polarization function were employed for H, C, and O atoms, while for Zr and Sm atoms triple-ζ STO basis sets with one p-type polarization function were employed. The 1s electrons of C and O, as well as the 1s−3d electrons of Zr and the 1s−4d electrons of Sm, were treated as frozen core. First-order scalar relativistic corrections were applied to the systems studied.[34−35,36]

The f electrons in the partially occupied 4f shell of Sm have required particular attention in order to ensure SCF convergence. Since in all the systems studied Sm is in the +3 oxidation state, an ionic Sm^{3+} ion fragment was created with a restricted calculation, in which a fractional, even occupation of the 4f orbitals was imposed (5 electrons in 7 orbitals). Therefore all calculations on systems containing Sm were based on atomic fragments, plus a Sm^{3+} ion fragment. Please note that the choice of fragments might help the SCF convergence, but it has no influence on the final outcome of the calculation.

Additionally, again to achieve SCF convergence, it was occasionally necessary to turn off the DIIS procedure[37] and to reduce the mixing parameter from the standard value to values ranging from 0.02 to 0.1.

All calculations were carried out in the gas phase without any symmetry constraint. Approximate transition states were located through reaction coordinate studies in which all degrees of freedom were minimized, while keeping a specific internal coordinate, or linear combination of internal coordinates, fixed. The leading coordinate for the backbiting reactions was the distance between the α-carbon of the enolate and the carbonyl carbon atom of the ester group involved in the reaction. For reactions in which transfer of a proton was involved, the reaction coordinate has been chosen as the length of the bond being broken minus the length of the bond being formed. In the case of the C−C coupling reaction the coordinate in question is the distance between the α-carbon of the enolate and the *β*-carbon of the acrylate. In the case of the ring-opening reactions, the chosen coordinate was the difference between the distances of the ligands (carbonyl oxygen of the incoming acrylate and carbonyl oxygen of the leaving ester group, respectively) from the metal center. All stationary points were then fully optimized as minima or transition states, starting from the constrained geometries. Our previous work[17] has shown that the systems under study are very floppy, especially the transition states in the ring-opening reactions, and frequency calculations have yielded a very high number of low-frequency modes. Under these conditions the harmonic oscillator approximation, under which vibrational frequencies are calculated, fails, thus affording unreliable values for the corrections to Gibbs free energies. For this reason frequency calculations have not been performed in this work, and reaction energies rather than free energies are reported throughout the paper.

Hybrid quantum-mechanical (QM) and molecular-mechanical (MM) models (QM/MM) have been applied to the modified catalysts described in the last part of this study, using the IMOMM scheme by Morokuma and Maseras,[38] as implemented in ADF by Woo et al.[39] The $-CH_2CH_2-$ bridge system and the alkyl substituents in the 3,4 and 3′,4′ positions were replaced by MM atoms, and H atoms were used to cap the QM system. The MM atoms were described using the SYBYL/TRIPOS 5.2 force field constants.[40]

No counteranion is present for the neutral samarocene system. Compared to the cationic zirconocene-catalyzed polymerization of olefins, the anion plays a much less important role in the GTP of acrylates, since the two available metal coordination sites are occupied at all times by oxygen-based strong *σ*-donor ligands and the anion, if existing, is always relegated to an outer shell. In light of such considerations, and in order to be able to compare more directly the results, the study with cationic zirconocenes was also conducted without considering the counteranion.

Discussion

Side Reactions Involving Eight-Membered Metallacycles. The eight-membered metallacycle formed in the coupling of the enolate and acrylate (**2**, Scheme 1) appears to be the resting state, as shown by theoretical and experimental studies.[1,3,15,26,27] Therefore, the first and most intuitive approach is to study the backbiting and the proton transfer events involving species like **2**. The backbiting reaction consists in the nucleophilic attack by the enolate α-carbon on the carbonyl carbon two monomer units away, i.e., the first free ester group on the polymer chain. The proposed mechanism amounts to a Dieckmann condensation (Claisen intramolecular condensation), and it leads to elimination of a MeOH molecule and formation of an unreactive product containing a substituted cyclohexanone ring, as illustrated in Scheme 2. Backbiting therefore causes termination of the polymerization process.

Similarly to the backbiting, the proton transfer involves the α-proton to the first free ester group on the polymer chain (see Scheme 3). The product of proton transfer is an internal enolate, which can potentially continue the polymerization process.

(27) Mariott, W. R.; Rodriguez-Delgado, A.; Chen, E. Y.-X. *Macromolecules* **2006**, *39*, 1318.
(28) te Velde, G.; Bickelhaupt, F. M.; van Gisbergen, S. J. A.; Fonseca Guerra, C.; Baerends, E. J.; Snijders, J. G.; Ziegler, T. *J. Comput. Chem.* **2001**, *22*, 931.
(29) Fonseca Guerra, C.; Snijders, J. G.; te Velde, G.; Baerends, E. J. *Theor. Chem. Acc.* **1998**, *99*, 391.
(30) ADF2004.01, SCM, Theoretical Chemistry, Vrije Universiteit, Amsterdam, The Netherlands (http://www.scm.com).
(31) Becke, A. D. *Phys. Rev. A* **1988**, *38*, 3098.
(32) Perdew, J. P. *Phys. Rev. B* **1986**, *33*, 8822.
(33) Perdew, J. P. *Phys. Rev. B* **1986**, *34*, 7406.
(34) Snijders, J. G.; Baerends, E. J.; Ros, P. *Mol. Phys.* **1979**, *38*, 1909.
(35) Boerrigter, P. M.; Baerends, E. J.; Snijders, J. G. *Chem. Phys.* **1988**, *122*, 357.
(36) Ziegler, T.; Tschinke, V.; Baerends, E. J.; Sijders, J. G.; Ravenek, W. *J. Phys. Chem.* **1989**, *93*, 3050.
(37) Pulay, P. *Chem. Phys. Lett.* **1980**, *73*, 393.
(38) Morokuma, K.; Maseras, F. *J. Comput. Chem.* **1995**, *117*, 5179.
(39) Woo, T. K.; Cavallo, L.; Ziegler, T. *Theor. Chem. Acc.* **1998**, *100*, 307.
(40) Clark, M.; Cramer, R. D. I.; van Opdenbosch, N. *J. Comput. Chem.* **1989**, *10*, 982.

Scheme 1. Mechanism for GTP Catalyzed by a Monometallic Cationic Zirconocene or a Monometallic Neutral Samarocene

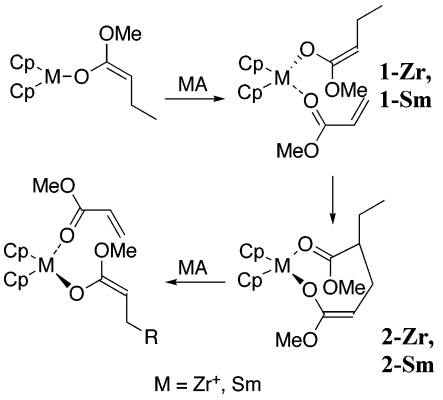

Scheme 2. Backbiting Reaction Mechanism

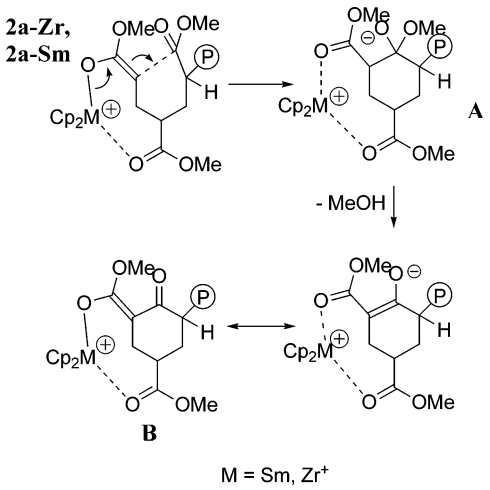

Scheme 3. Proton Transfer Reaction

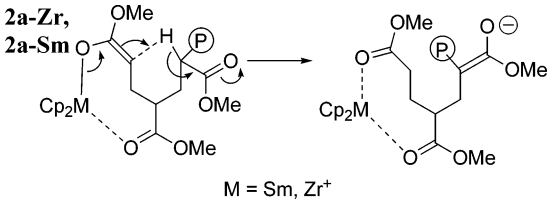

The two reactions have been studied for the neutral samarocene as well as for the cationic zirconocene. For both systems several configurations of **2** are possible, depending on the conformations of the metallocene-enolate-acrylate complexes (**1**) that generated them. In a previous publication[17] we have shown that Cp_2M(MA)(enolate) complexes (**1** in Scheme 1, M = Sm, Zr^+) can exist in four possible conformations, consisting of two enantiomeric pairs, and that the configuration of the newly formed stereocenter is determined by the enantiotopic face of the enolate involved in the coupling reaction. It is in addition necessary to take into account only one configuration of each enantiomeric pair to fully describe the coupling process. Also, given that in the coupling the acrylic moiety is transformed into an enolate, the configuration of the stereocenter formed in the following coupling event depends on the orientation of MA in the original complex. Each metallacycle can generate two new diasteromeric reacting complexes, depending on the orientation of the incoming MA in the ring-opening reaction. There are therefore not four, but eight possible diasteromeric reacting complexes, constituting four enantiomeric pairs, leading to four enantiomeric pairs of the corresponding metallacycles.

Four diasteromeric metallacycles **2a-Zr** (one from each enantiomeric pair), corresponding to the product of the second coupling reaction, have been optimized for the cationic Zr-based system and two for the neutral Sm-based system **2a-Sm**. The difference in energy between the diasteromeric forms of **2a** is not large; the formation energies relative to the respective THF precatalyst complex range from −64.8 and −68.2 kcal/mol in the case of **2a-Zr** to −71.0 and −72.8 kcal/mol in the case of **2a-Sm**, as reported in Table 1.

A closer inspection of the structures obtained from the calculations on **2a-Zr** reveals that the geometries in which the methoxy groups are on the same side of the metallacycle (*down/down* structures) have conformations that do not permit bringing the ester group of the side chain close enough for the enolate to react, without inflicting considerable strain (structures of the diasteromers of **2a-Zr** are shown in Figure 1). For this reason only the two geometries capable of undergoing the reaction were optimized for the more computationally expensive **2a-Sm**.

Because of the considerations given above, the backbiting and the proton transfer have been studied only for the "up/down" **2a-Zr** with *S*,*S* and *S*,*R* configurations and the equivalent "down/up" **2a-Sm** having *R*,*R* and *R*,*S* configurations. Exploring a reaction mechanism for different diasteromers of the same type of metallacycle corresponds to studying that reaction for a *syndio*-like (alternating chiral centers) or an *iso*-like polymer (stereogenic centers of same chirality).

Backbiting Reaction in Zr- and Sm-Eight-Membered Metallacycles. The backbiting reaction mechanism is depicted in Scheme 2; it occurs in the same way for the neutral samarocene metallacycle and the cationic zirconocene metallacycle. The reaction consists of two steps, first a C−C coupling, in which a six-membered ring is formed (tetrahedral intermediate **A**), likely followed by MeO^- elimination. This elimination is an unfavorable equilibrium in the classic Claisen condensation, in which the system is negatively charged, so it can be expected to be even more so in a neutral system, like the neutral samarocene, or in a positively charged system like the cationic zirconocene. In the Claisen condensation, the equilibrium is driven by the deprotonation of the product. The difference between MMA and MA is that only MA has a α-proton, which can possibly be eliminated, at least to some extent, in a concerted manner, lowering the energy barrier in the elimination step and stabilizing the product.

We have not found a stationary point on the potential energy surface corresponding to the tetrahedral intermediate **A**. It would be expected that the energy of the system increases as the molecule changes conformation in order to bring the nucleophile and the electrophile at reacting distance, until at a certain C−C separation an energy maximum (the transition state) is attained, after which the energy decreases and an intermediate product is generated. However, no stationary point corresponding to a transition state has been found for the down/up *S*,*S* and down/up *S*,*R* **2a-Zr** (see Figure 2). The decrease in energy that can be seen in both curves at shorter C−C separations is due to the interaction between the negatively charged carbonyl oxygen of the ester group involved in the backbiting and the carbonyl carbon of the ester group coordinated to the metal center. Such high-energy structures revert to the reactants when the geometrical constraint used for exploring the reaction is released.

The backbiting products containing the cyclohexanone ring (intermediate **B** in Scheme 2) have been optimized for both selected configurations of the Zr-based system. In both cases

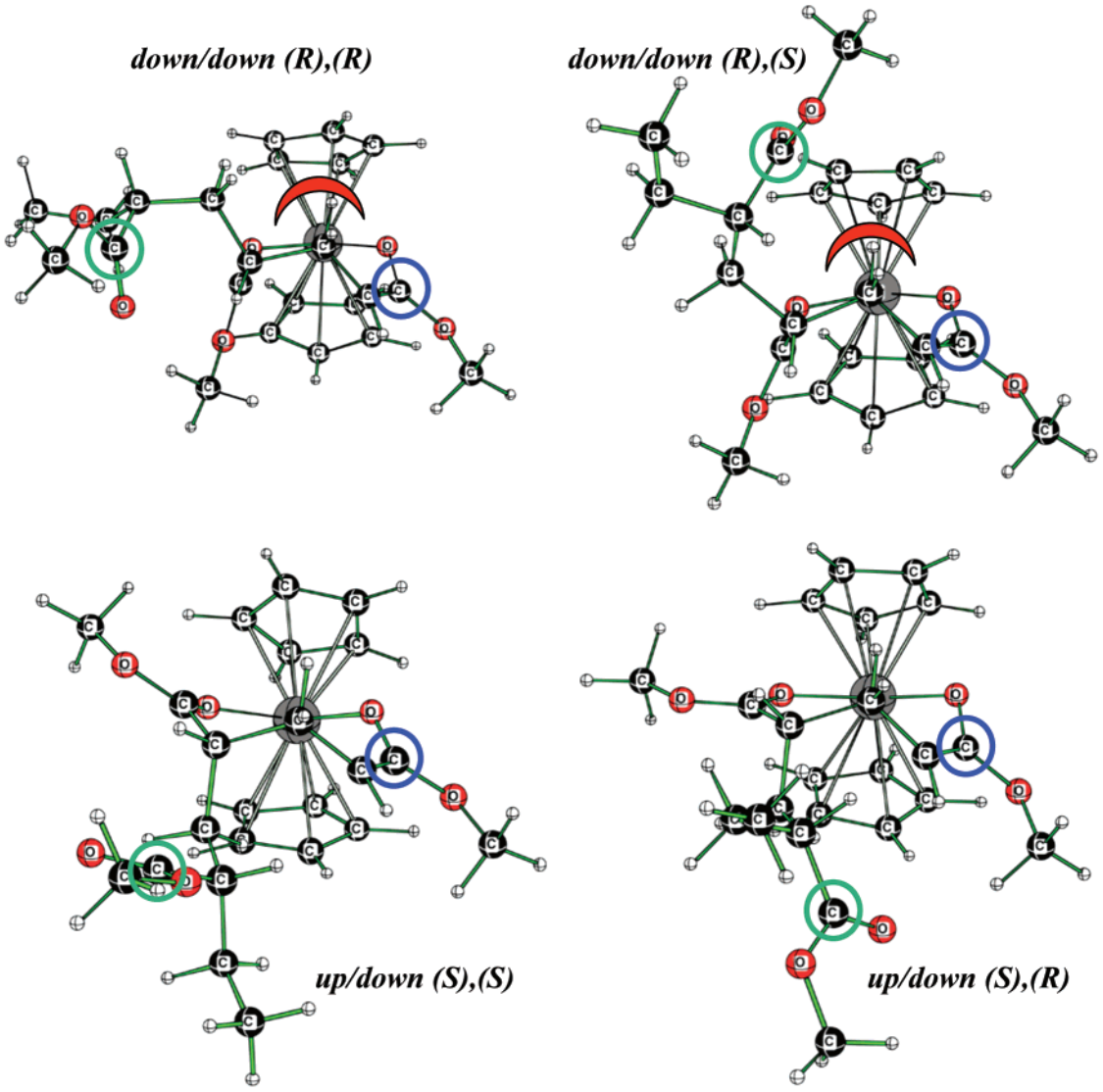

Figure 1. Diasteromeric zirconocene metallacycles (**2a** in Scheme 2) obtained after the second monomer addition. Carbon atoms circled in green are the electrophile in the backbiting reaction; those circled in blue are the nucleophile. The red crescent indicates that the backbiting reaction cannot occur for steric reasons. See text for details. Energies are shown in Table 1.

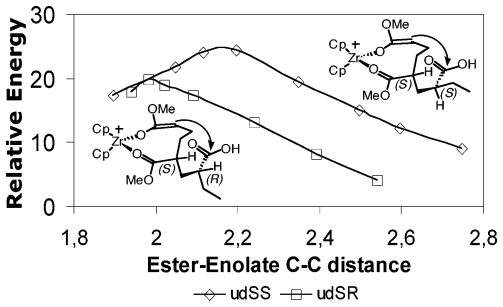

Figure 2. Backbiting reaction profile in the cationic Zr-based system.

they are high-energy intermediates, 12.9−13.2 kcal/mol less stable than the parent metallacycles **2a-Zr** ("up/down" *S*,*R* and "up/down" *S*,*S*, respectively); no direct reaction path connecting them to the parent eight-membered metallacycle has been found.

The bond lengths (reported in Table 2) show that the ketone C═O double bond and the other C−C and C−O bonds connecting to the metal center through the enolate ligand are intermediate between typical single and double bond distances, indicating resonance between the two canonical forms represented in Scheme 2.

Table 1. Energies of Samarocene and Zirconocene Metallacycles (2a in Scheme 2), Obtained after the Second Monomer Addition[a]

metallacycle	E_{rel}[b]
2a-Zr -dd-(*R*),(*R*)[c]	−68.2
2a-Zr-dd-(*R*),(*S*)	−64.8
2a-Zr-ud-(*S*),(*R*)[d]	−67.5
2a-Zr-ud-(*S*),(*S*)	−67.3
2a-Sm-du-(*R*),(*R*)[e]	−71.0
2a-Sm-du-(*R*),(*S*)	−72.8

[a] The reference Zr and Sm species are Cp_2ZrMe^+THF and $Cp_2SmMeTHF$, respectively. [b] Relative energies in kcal/mol. [c] "dd" = "down/down". [d] "ud" = "up/down". [e] "du" = "down/up".

Likewise, the energy of the system for the backbiting in **2a-Sm** shows no maximum as C−C separation decreases (see Figure 3).

Also in the case of **2a-Sm**, the backbiting products containing the cyclohexanone ring (structure **B** in Scheme 2), obtained after elimination of a MeOH molecule, are local minima, albeit 10.1−11.0 kcal/mol less stable than the parent **2a-Sm** ("down/up" *R*,*S* and "down/up" *R*,*R*, respectively). The bond lengths in Table 2 show that there is a delocalized system connecting the Sm metal center to the ketone C═O bond.

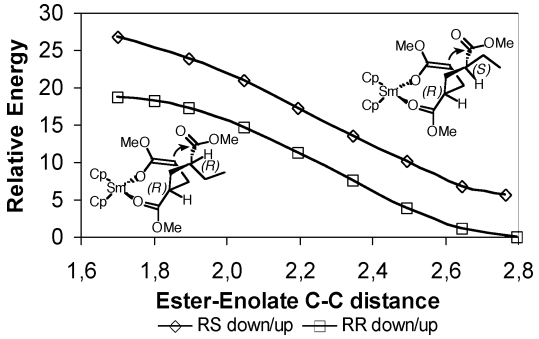

Figure 3. Backbiting reaction profile in the neutral Sm-based system.

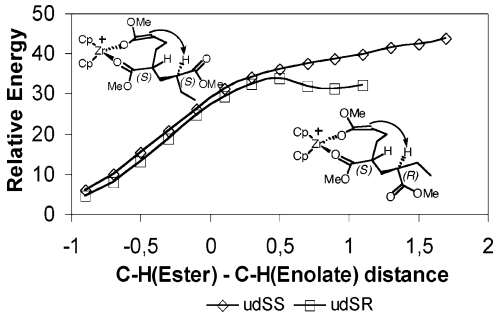

Figure 4. Energy profile for the proton transfer in the Zr-based system.

Table 2. Selected Interatomic Distances for the Backbiting Intermediate Containing the Cyclohexanone Moiety (species B in Scheme 2)[a]

species	C═O(ket)	C−C$_\alpha$	C═C	C−O	O−Zr
Zr$^+$-ud-(*S*),(*R*)[b]	1.24	1.45	1.39	1.33	2.08
Zr$^+$-ud-(*S*),(*S*)	1.24	1.46	1.42	1.30	2.15
Sm-du-(*R*),(*R*)[c]	1.25	1.43	1.41	1.29	2.26
Sm-du-(*R*),(*S*)	1.25	1.44	1.41	1.29	2.29

[a] The backbiting mechanism is illustrated in Scheme 2. [b] "ud" = "up/down". [c] "du" = "down/up".

Although no defined transition state has been characterized, it is quite obvious that transition states and products in the backbiting process involving the enolate moiety in the eight-membered metallacycle and a nonactivated ester group on the polymer chain will be electronically and sterically destabilized, making the process at least very slow and not competitive with the propagation.

Proton Transfer in Zr- and Sm-Eight-Membered Metallacycles. The proton transfer reaction involves the proton in the α-position to the ester of **2a**, instead of the ester C═O bond involved in the backbiting reaction. A six-membered transition state, with the α-H being part of such a ring, is expected to be formed, as depicted in Scheme 3.

The transfer of the ester α-proton to the enolate α-carbon was studied from the same starting geometries used for the study on backbiting, namely, the "up/down" **2a-Zr** with *S,S* and *S,R* configurations and the "down/up" **2a-Sm** with *R,R* and *R,S* configurations.

For the up/down, *S,S* **2a-Zr**, transferring the ester α-proton to the enolate α-carbon resulted in a monotonic increase in energy. For the other geometry ("up/down", *S,R*), a very shallow local minimum was found on the constrained linear transit coordinate (see Figure 4). In both cases, the end point of the linear transit, in which the C−H bonds and carbon hybridations have been swapped, is more than 30 kcal/mol above the reactant and spontaneously reverts to the starting point when it is optimized freely.

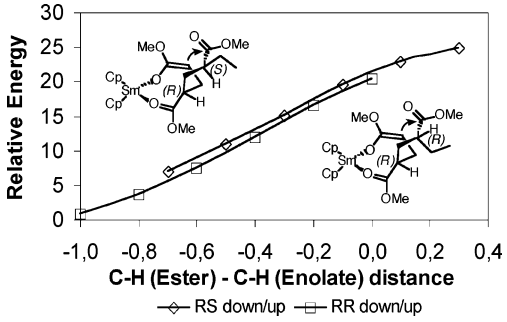

Figure 5. Energy profile for the proton transfer in the Sm-based system.

The possibility that the ester group enolizes before the proton is transferred from the oxygen atom to the enolate α-carbon has been investigated for the Zr-based system. Formation of the enol is endothermic by 25.8 kcal/mol.

A similar approach was adopted to study the linear transit for the proton transfer from the enol form of the ester. The end point of the linear transit, which is very similar in geometry and in energy to the proton transfer linear transit end point from the ester form, also reverts spontaneously to the most stable form of the reactant (the ester form) when reoptimized without geometrical constraints.

Similar results were obtained for **2a-Sm** (see Figure 5).

The lack of a transition state for the proton transfer and most of all the spontaneous return to the reactant state show that, as for the backbiting, there are electronic and steric factors, which greatly inhibit the proton transfer, especially in comparison with the propagation.

10-Membered Metallocenes. The importance of activating the ester group, i.e., enhancing its electrophilic character, appears to be critical for the feasibility of the backbiting and of the proton transfer reactions. The electron-withdrawing effect of a cation coordinated to the ester group, like the metallic center, could activate it sufficiently, but the eight-membered metallacycle **2a** is not flexible enough to accommodate the displacement required for the backbiting reaction, while the cumulated six-membered and four-membered ring system that would result from the reaction would highly strain the product. Furthermore, the proton transfer would be altogether not possible since the active α-H is facing outward from the metallacycle.

It is possible however, and especially as the concentration of free MA decreases, that the first ester group of the polymer chain competes with MA in the ring-opening reaction, displacing the ester group of the metallacycle and forming a larger 10-membered metallacycle (**3** in Scheme 4).[27] A 10-membered metallacycle could better meet the requirements of conformational freedom necessary for the backbiting to occur, and the hypothetical backbiting product would benefit thermodynamically from the formation of a bicyclic, cumulated, system of six-membered rings.

The conversion of the *S,S* up/down **2a-Zr** into the 10-membered metallacycle **3-Zr** is exothermic by 1.3−5.0 kcal/mol, depending on the conformation of the product (see Table 3). A conformational equilibrium gives access to the more stable conformation **3b-Zr**, which is capable of undergoing easily (internal activation energy: 12.5 kcal/mol, 7.5 kcal/mol higher than the parent eight-membered metallacycle, see Table 3) and exothermically the first step of the backbiting reaction, to afford a tetrahedral intermediate **4a-Zr**, as represented in the second reaction of Scheme 4. **4a-Zr** resembles the less stable conformer of **3a-Zr**, and the conformation of the six-membered ring is that of a slightly twisted boat. A conformational equilibrium

Scheme 4. Backbiting and Decomposition in 10-Membered Metallacycles

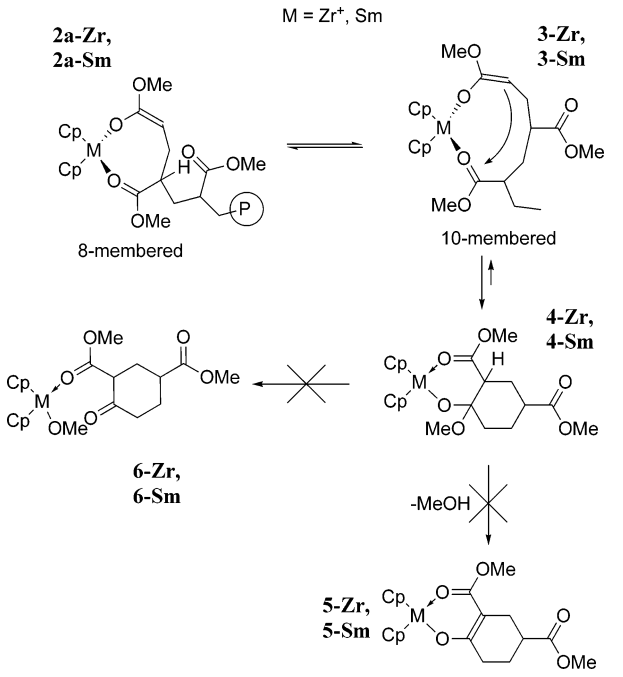

Table 3. Energies of the Species Involved in the Backbiting Reaction of the Cationic Zirconocene 10-Membered Metallacycle 3-Zr

species	E_{rel}[a]
3a-Zr	−1.3
3b-Zr	−5.0
3b-Zr TS	7.5
4a-Zr (boat)	−2.9
4b-Zr (chair)	−9.5
5-Zr	−15.0

[a] All energies are relative to the parent eight-membered metallacycle **2a-Zr** in "down/down" conformation. Relative energies in kcal/mol.

leads to another conformation, **4b-Zr**, more stable by 6.6 kcal/mol (9.5 kcal/mol more stable than **2a-Zr**), in which the six-membered ring has a chair conformation. The energies of the species along the reaction coordinate are shown in Figure 6. This more stable conformation of the tetrahedral intermediate resembles that of **3b-Zr**, although no direct reaction channel connecting the two has been searched.

The tetrahedral intermediate **4b-Zr** is then potentially capable of undergoing different reactions that irreversibly give stable products. One of them involves elimination of MeOH to yield a stable cationic zirconocene acac-type complex, **5-Zr**. Thermodynamically the reaction is favorable (5.5 kcal/mol exothermic from **4b-Zr** and 15.0 kcal/mol from **2a-Zr**, see Figure 6) and the reverse process is less likely because, in addition to a barrier higher than that of the forward process, it is also disfavored by entropy. Two mechanisms have been considered for the elimination of a molecule of methanol from the backbiting tetrahedral intermediate **4b-Zr**. The first possibility is that a concerted elimination occurs, during which the C−H and MeO−C σ-bonds are broken, while a σ O−H bond and a π C−C bond are formed, likely not in an isochronous way.

Different approaches have been adopted to find a transition state for a concerted elimination. In all cases, the reaction energy profile rises to more than 30 kcal/mol above the reactant, without meeting a transition state.

The second mechanistic possibility is that a two-step elimination occurs, following an E1cB mechanism. Abstraction of a

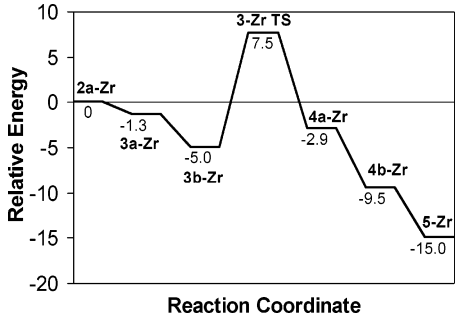

Figure 6. Species along the reaction coordinate from the eight-membered metallacycle to the backbiting product after elimination of a MeOH molecule. The energies are in kcal/mol, relative to the eight-membered metallacycle.

proton from the tetrahedral intermediate is easy (exothermic, barrierless process) in the presence of a sufficiently strong base, such as a methoxy group (eliminated from another molecule or tetrahedral intermediate). However, the calculations have shown that elimination of a MeO^- group from the neutral deprotonated product also requires a very high activation energy (more than 30 kcal/mol), which makes MeOH elimination not viable.

Another possibility is that the methoxy group in the tetrahedral intermediate **4b-Zr** is transferred to the Zr center. The process should be irreversible due to the strength of the Zr−OMe bond of **6-Zr**, but also the transfer of MeO^- to Zr has a very high activation energy (>30 kcal/mol).

Therefore the backbiting product intermediate from **3b-Zr** can be obtained quite easily and is lower in energy than the eight-membered metallacycle **2a-Zr** involved in chain growth, but the process is not irreversible. Transformation to a 10-membered metallacycle and subsequent backbiting therefore are likely to trap the propagating center, greatly slowing chain propagation and causing it to be not living (as experimentally observed), but do not necessarily lead to termination.

Proton transfer in **3b-Zr** has not been studied. As with eight-membered metallacycles, in both conformations the α-H points out of the ring, making transfer to the enolate α-carbon on the opposite side of the ring not viable.

Polymer Chain Transfer Reactions. Similarly to the formation of a 10-membered metallacycle from the eight-membered one, larger metallacycles can be obtained by displacing the metallacycle ester group with ester groups farther away in the polymer chain. In the limit of an infinitely far ester group, a new type of cationic zirconocene (or neutral samarocene) ester/enolate complex **7** can be formed, which can be considered not to be a metallacycle (see Scheme 5). Also, it can be assumed that metallacycle opening with a very remote ester group situated on the growing polymer or on another polymer chain are equivalent in terms of activation entropy.

As MA is consumed as a result of the polymerization process, its concentration drops and that of polymer chain ester groups soars, making this reaction increasingly more competitive with the MA-assisted ring opening described in previous reports.

The bonding of a model representing a polymer ester group (i.e., $CH_3CH(COOMe)CH_3$) to the metallacycle has been compared to that of the metallocene-MA-enolate complexes **1** (M = Zr, Sm). The complexation of the polymer model to the metallocenium enolate is more exothermic than the complexation of MA by 7.3−12.1 kcal/mol (**7a-Zr**) and 7.4−12.7 kcal/mol (**7a-Sm**) (see Table 4).

The complexes so obtained have an ester group activated by the metal, capable of reacting intramolecularly with the enolate α-carbon. Since the shortcomings of the backbiting reaction

Scheme 5. Polymer Chain Transfer Reaction Mechanism

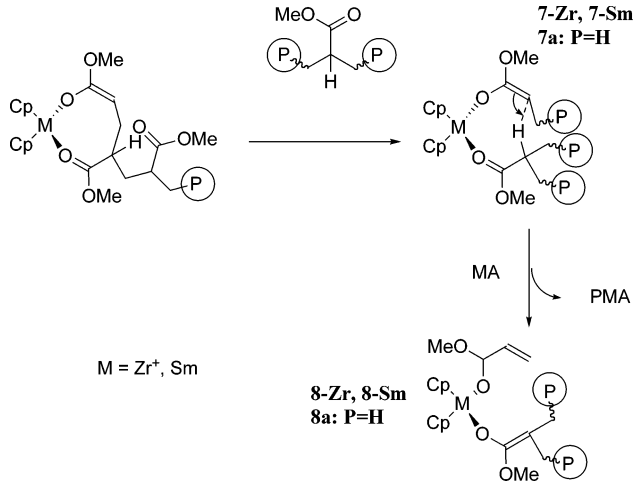

Table 4. Comparison of Formation Energies of Samarocene and Zirconocene Enolate-MA Complexes (1, Scheme 1) with Samarocene and Zirconocene Enolate-Polymer Model Complexes (7a, Scheme 5)

species	E_{rel}[a]
1-Zr "down/up"	−25.4
1-Zr "down/down"	−30.2
7a-Zr "down/up"	−39.7
7a-Zr "down/down"	−39.1
1-Sm "down/up"	−38.4
1-Sm "down/down"	−39.0
7a-Sm "down/up"	−51.1
7a-Sm "down/down"	−46.4

[a] Energies are relative to the precatalyst THF complex. Relative energies in kcal/mol.

were already known (i.e., difficult formation of an irreversible product because of the high energetic cost for the cleavage of the C−OMe bond), the transfer of a proton has been studied instead. The proton transfer in this case has no conformational restraints. As shown in Scheme 5, the product of proton transfer is a new enolate/ester metallocene complex **8**, but the enolate is internal, and therefore it could be less reactive. Chain propagation is at least slowed and growth on the polymer chain is stopped and transferred to the α-position of an ester group (the new, internal enolate), resulting in chain branching. Indeed, this reaction has been exploited in some cases, in which active hydrogen compounds such as thiols or enolizable ketones have been employed as chain transfer agents.[41−43]

The chain transfer reaction has been studied first for simple biscyclopentadienyl Zr- and Sm-based systems **7a-Zr** and **7a-Sm**.

In the case of **7a-Zr**, the "down/down" and "down/up" complexes (equivalent to the Cp_2Zr^+enolate−MA complexes **1-Zr**) have been used as starting points for the study of the reaction coordinate describing the transfer of the α-H to the enolate. Before other major changes in the geometry occur, the polymer model ligand rotates in order to align the C−H bond as perpendicular as possible to the π-plane of the enolate. This process hardly involves any change in energy, and its result is the same for both starting geometries; that is, there is just one transition state for the proton transfer, which is common for

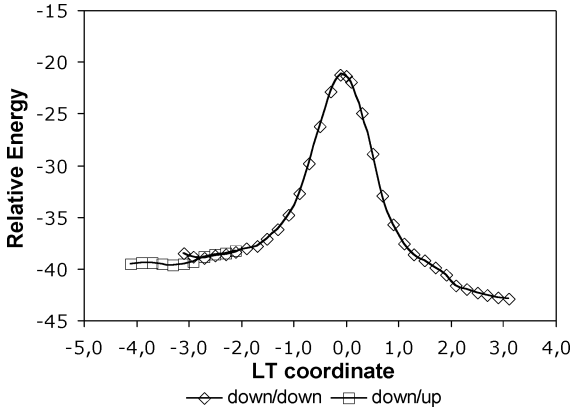

Figure 7. Chain transfer energy profile for **7a-Zr** of "down/down" and "down/up" conformations. The reference Zr species is Cp_2ZrMe^+THF.

Table 5. Effect of Catalyst Modifications on the Energies of Local Minima in the Chain Transfer Reaction Involving Samarocene and Zirconocene Enolate-Polymer Model Complexes 7[a]

species	TS	product
7a-Zr dd[b]	17.2	−3.9
ansa/Me **7a-Zr** dd	21.4	
ansa/*i*-Pr **7a-Zr** dd	31.2	
7a-Sm dd	12.7	−4.0
7a-Sm du	16.9	0.7
Cp* **7a-Sm** dd	23.7	

[a] Internal activation energies and reaction energies are relative to the ester-enolate metallocenium complexes of the respective geometry ("down/down" or "down/up"). The **7a-Sm** "down/up" complex with simple Cp ligands is 4.7 kcal/mol more stable than the "down/down" complex, while the difference at the TS is redced to 0.5 kcal/mol. Relative energies in kcal/mol. [b] dd = "down/down".

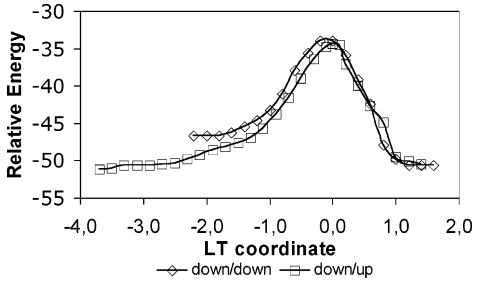

Figure 8. Chain transfer energy profile for **7a-Sm** of "down/down" and "down/up" conformations. The reference Sm species is $Cp_2SmMeTHF$.

the two starting geometries. The internal barrier for the process (see Figure 7 and Table 5) is 17.2 kcal/mol for the "down/down" complex and 17.8 kcal/mol for the "down/up" one, because of the different stability of the starting complexes. The product is more stable than the "down/down" reactant by 3.9 kcal/mol.

Chain transfer has higher activation energy than the C−C coupling in the backbiting reaction. Therefore it is likely that chain transfer is slower than backbiting, in agreement with recent work by Chen and co-workers,[27] according to which backbiting is the sole origin for termination products.

For **7a-Sm**, the internal barriers (Figure 8 and Table 5) are 12.7 and 16.9 kcal/mol (from the "down/down" and "down/up" geometries, respectively). Also in this case, the TSs are very close in geometry and energy. The reaction from the "down/down" complex is exothermic by 4.0 kcal/mol, while the reaction from the "down/up" complex, which is more stable, is nearly thermoneutral.

(41) Nodono, M.; Tokimitsu, T.; Tone, S.; Mskino, T.; Yanagase, A. *Macromol. Chem. Phys.* **2000**, *201*, 2282.
(42) Lian, B.; Toupet, L.; Carpentier, J.-F. *Chem.−Eur. J.* **2004**, *10*, 4301.
(43) Lian, B.; Lehmann, C. W.; Navarro, C.; Carpentier, J.-F. *Organometallics* **2005**, *24*, 2466.

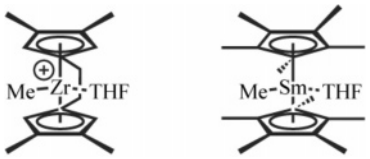

Figure 9. Bulkier systems used in the study of the minimization of side reactions.

Therefore, according to these calculations, it seems that Sm is not inherently a better metal than Zr in terms of reducing chain transfer. The better results obtained polymerizing acrylates with Sm-based systems, compared to Zr-based systems, must be due to the increased steric bulk caused by the Me substituents of the Cp* ligands. Yasuda's systems are permethylated, while most of the Zr-based systems, even the *ansa* ones, do not have as much steric hindrance on the coordination sites for the oxygen-based ligands.

A proper comparison of the experimentally used samarocenes and zirconocenes requires studying the chain transfer for the pentamethylated samarocene while changing the basic zirconocene to a more complex system, with substituents on the front region. Such a comparative study could give information on whether it is possible to reduce side reactions through steric modifications on the ligands.

Minimization of Side Reactions. To minimize a side reaction, it is necessary to increase its activation energy compared to that of the propagation, which can be achieved through modifications to the catalyst that selectively destabilize the transition states for the backbiting and chain transfer reactions, thus slowing the side reactions more than the propagation. Modifications to the catalyst should ideally slow the side reactions, while not affecting adversely the propagation steps.

In both transition states for the backbiting in the 10-membered metallacycle **3** and the chain transfer, the side groups of the enolate and ester ligands are roughly parallel to the plane formed by the metal center and the Cp centroids. This orientation brings them closer to the protons of the Cp rings than they are at the beginning of the reaction. Bulkier groups in the positions of the Cp rings that are closest to the ligands are likely to increase steric repulsions in the transition state, thus slowing this side reaction. To prove that, the reaction was explored again with bulkier substituents on the Cp rings.

For the Sm system, the real, permethylated system used by Yasuda has been studied, while in the case of the cationic Zr system, a 3,4,3′,4′-tetramethylated *ansa* (CH_2-CH_2 bridge, as in the bis-indenyl system used by Chen and co-workers,[27] which has been proven to be an effective mononuclear zirconocenium catalyst for the GTP of methyl methacrylate) system ("*ansa/Me*") has been selected (Figure 9). Due to the increased size of the system, this part of the study has been carried out mostly using hybrid QM/MM calculations, in which the QM core corresponds to the smaller systems studied previously and the MM part to the substituents introduced on the Cp rings.

Preliminary full QM calculations have been conducted for the initiation step and the enolate-acrylate complexes. The energies of these species are reported in Table 6. The equivalent structures for the systems with simple Cp ligands have been reported in our previous paper.[17]

For both Sm- and Zr-based precatalyst THF complexes, abstraction of THF in the larger systems is easier than with simple Cp rings, by 4.7 kcal/mol in the case of the neutral samarocene and 6.3 kcal/mol for the cationic zirconocene. This is indicative of a weaker interaction between the metal center and the THF oxygen atom, as witnessed by an increase of the O−M distance (M = Sm, Zr^+). Likewise, in the real systems the generation of the enolate is slightly less exothermic (by 3.8 kcal/mol for Zr and 0.4 kcal/mol for Sm).

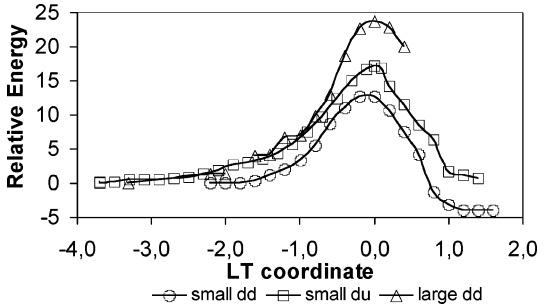

Figure 10. Comparison of chain transfer reaction profiles for differently substituted samarocenes. The lowest point in the left side (reactants) of each curve is assigned 0 relative energy. The small system has Cp ligands; the large one has Cp*.

Table 6. Energies of Samarocene and Zirconocene Species (large systems, full QM calculations)

species	E_{rel}[a]
Et-Cp^+_2ZrMeTHF$^+$	0
Et-Cp^+_2ZrMe$^+$	35.1
Et-Cp^+_2ZrMeMA$^+$	1.4
Et-Cp^+_2ZrEno$^+$	−12.0
Zr-down/down complex	−24.0
Zr-down/up complex	−28.9
Cp^*_2SmMeTHF	0
Cp^*_2SmMe	13.8
Cp^*_2SmMeMA	3.8
Cp^*_2SmEno	−32.8

[a] Relative energies in kcal/mol.

Calculations on the **Cp*-1-Sm** complexes have revealed no stable complexes of this kind. Instead, the complexes (whose initial geometries were obtained from the small systems, by adding Me groups) evolved during the calculation to the corresponding coupling product, i.e., the eight-membered metallacycle **Cp*-2-Sm**. This is caused by the methyl groups on the Cp* rings: the steric repulsion between the Me substituents and the acrylate and enolate ligands brings the enolate α-C and the acrylate *β*-C close enough for the coupling to occur spontaneously.

In the case of the modified *ansa-Me* Zr-based system, stable ***ansa-Me* 1-Zr** complexes have been found. Their formation energies (from the cationic THF complex precursor) are on average 1 kcal/mol less favorable than for the smaller **1-Zr** complexes.

The effect of the substitution on the chain transfer side reaction has been investigated performing linear transit calculations, which show that the internal activation energy required to transfer the proton increases as bulkier groups are introduced on the 3,4 and 3′,4′ positions.

In the case **Cp*-7a-Sm**, the barrier for the faster chain transfer reaction channel is increased by 11.0 kcal/mol compared to **7a-Sm** (see Figure 10 and Table 5).

This is in agreement with the better results obtained experimentally in the GTP of acrylates catalyzed by Yasuda's neutral samarocene, compared with those catalyzed by cationic zirconocenes, which suffer more from side reactions.

The modification chosen for the cationic zirconocene is not as effective in raising the energy of the chain transfer as the Cp* ligand is for the neutral samarocene, as witnessed by an increase of the barrier of just 4.2 kcal/mol, from 17.2 kcal/mol to 21.4 kcal/mol (see Figure 11 and Table 5). Only two methyl

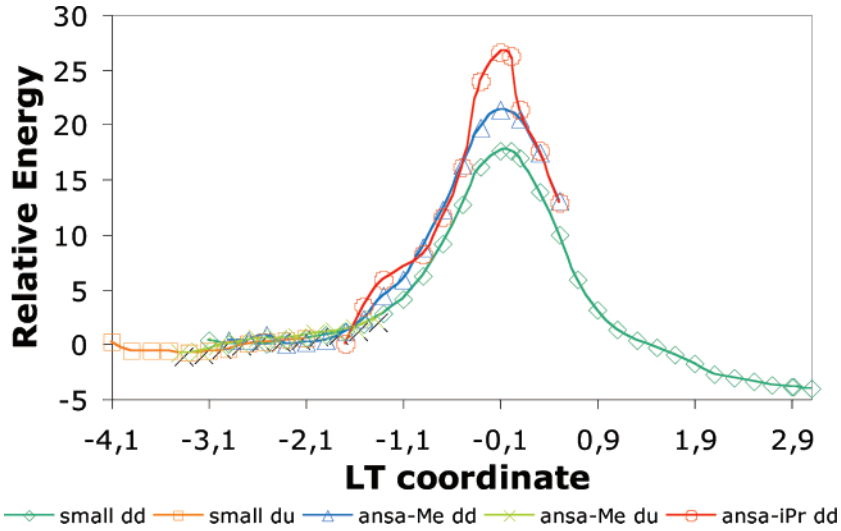

Figure 11. Comparison of chain transfer reaction profiles for differently substituted zirconocenes. The lowest points in the left side (reactants) of the "dd" curves are assigned 0 relative energy.

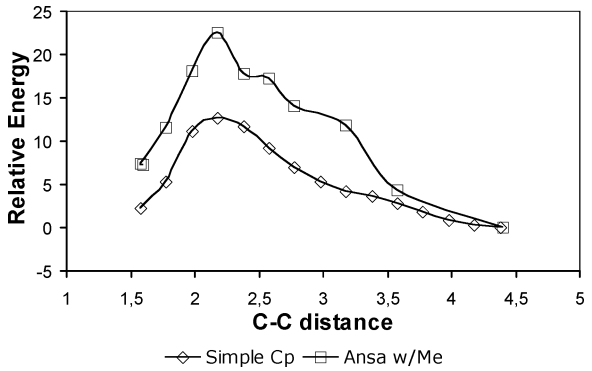

Figure 12. Comparison of backbiting reaction profiles for differently substituted 10-membered zirconocenium metallacycles **3b** ("up/down" *S*,*S* diasteromer). The 10-membered metallacycle start points are assigned 0 relative energy.

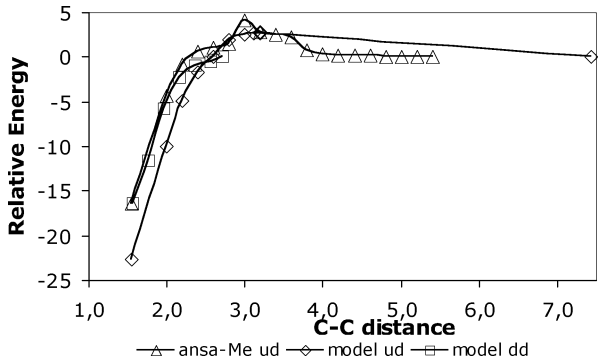

Figure 13. Comparison of C−C coupling reaction profiles for differently substituted **1-Zr** ("up/down" geometry). The respective reacting complex start points are assigned 0 relative energy.

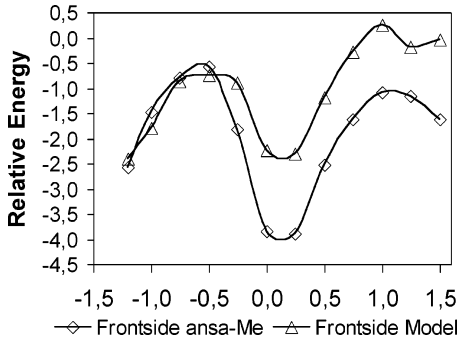

Figure 14. Effect of catalyst modification on the frontside MA-assisted ring-opening reaction profile for **2-Zr** ("down/down" metallacycle). The respective metallacycle start points are assigned 0 relative energy.

groups per Cp ring do not exert an effect as strong as that found with Cp*, as could also be inferred by the fact that the acrylate-enolate complexes are stable species.

Further bulking up the front coordination sites with *i*-Pr groups instead of Me groups ("*ansa/iPr*") increases further the internal activation energy for the chain transfer in ***ansa/iPr*-7a-Zr**, increasing it to 31.2 kcal/mol, 14.0 kcal/mol more than that obtained with **7a-Zr** (simple Cp ligands). The increase of the barrier by 4.2 kcal/mol with ***ansa/Me*-7a-Zr** is however already quite effective in reducing the incidence of the chain transfer, and further calculations show that this system is even better in inhibiting the backbiting in the 10-membered metallacycle, which is more facile than the chain transfer and therefore more important. While the barrier for the backbiting is 12.5 kcal/mol with **3b-Zr**, ***ansa/Me*-3b-Zr** has a barrier of 22.5 kcal/mol (see Figure 12). A further increase in the steric bulk (i.e., substituting the *i*-Pr groups with *t*-Bu ones) would probably further increase the barrier, but could affect negatively the propagation steps.

The possible effects of the modification to the catalyst on the key steps for propagation, i.e., C−C coupling and ring opening, were assessed by reoptimizing some of the curves for these processes that were computed in our previous work. The structures corresponding to linear transit points of selected reaction energy profiles were reoptimized after introducing the necessary modifications to the catalyst system, while holding fixed the value of the reaction coordinate. There are only minor changes in the C−C coupling reaction profile of **1-Zr**, "up/down" complex, as shown in Figure 13.

Also in the frontside ring-opening reaction of the "down/down" cationic zirconocene metallacycle **2-Zr**, i.e., the reaction path that leads to the alternating syndio product, the energies of the approximate transition states, relative to the parent metallacycle plus MA, do not change much, although their ordering does (see Figure 14).

This last fact would require a less approximate treatment of kinetics than that previously published[17] in order to predict stereoselectivity, although this is beyond the scope and the objectives of this publication.

Conclusions

Through this DFT study, we have explored the mechanism of termination and transfer reactions in the group transfer polymerization of methyl acrylate, catalyzed by cationic or neutral d-block or f-block monometallic metallocenes.

No competitive side reactions are possible from the eight-membered metallacycle resting state **2a**, for both the neutral Sm-based and the cationic Zr-based system.

An isomerization of the eight-membered metallacycle **2a-Zr** to the 10-membered metallacycle **3-Zr** is possible and slightly exothermic. The importance of this reaction could increase as the concentration of the monomer decreases. **3b-Zr** easily undergoes backbiting to yield a stable tetrahedral intermediate, whose formation however is not coupled to an irreversible reaction. The lower energy of the intermediate **4b-Zr** compared to **2a-Zr**, the higher barrier for the backbiting reverse process, together with the reduced concentration of the monomer in more advanced stages of the polymerization, could however trap enough of the propagating centers and effectively bring chain growth to a halt.

Ring opening from ester groups in more remote locations of the polymer chain, and possibly on other polymer chains, is also increasingly competitive with MA-assisted ring opening as the polymerization proceeds. The resulting metallocenium polymer-enolate complexes **7** can undergo chain transfer, killing the growing chain and transferring the propagation center to a different position, thus creating a branching and increasing polydispersity.

Minimization of these two processes can be achieved with a cationic zirconocenium catalyst by bulking up the Cp rings in such a way that the transition states for backbiting in the 10-membered metallacycle and polymer chain transfer are destabilized. It has been shown that the modified *ansa* system (C_2H_4-bis(3,4-diMe-Cp) ligand) is capable of addressing this need while at the same time not affecting adversely the key steps of propagation.

Acknowledgment. This work has been supported by BASF. T.Z. thanks the Canadian government for a Canada Research Chair in theoretical inorganic chemistry. The authors are grateful to E.-X. Chen for the useful discussions and for disclosing data on acrylate polymerizations still unpublished when the research was ongoing.

OM061058A